

Research Article | Araştırma Makalesi

ELECTRONIC AND TOPOLOGICAL INVESTIGATION OF ANTITUBERCULAR TRYPTANTHRIN ANALOGUES AND THEIR INTERACTION WITH THE ENOYL-ACP REDUCTASE USING IN SILICO METHODS

ANTİTÜBERKÜLOZ TRIPTANTRİN ANALOGLARININ ELEKTRONİK VE TOPOLOJİK ÖZELLİKLERİNİN VE ENOİL-ACP REDÜKTAZ İLE ETKİLEŞİMLERİNİN İN SİLİKO YÖNTEMLERLE İNCELENMESİ

  Fatma Aksakal*

*Department of Analytical Chemistry, Faculty of Pharmacy, Kocaeli Health and Technology University, Kocaeli, Türkiye.



Abstract

Objective: This study aimed to investigate the structure-antitubercular activity relationships of a series of tryptanthrin analogues and the binding mechanisms of these analogues with InhA, *Mycobacterium tuberculosis* enoyl-acyl carrier protein (enoyl-ACP) reductase.

Methods: Firstly, pharmacophores and anti-pharmacophores have been determined with the Electronic-Topological Method (ETM) and activity prediction models have been developed with the ETM-Neural Networks (NN) approach. In the second step, the binding affinities and conformations of the compounds to the InhA enzyme and noncovalent interactions between them were investigated with the molecular docking method. Finally, these interactions were discussed with the electron density distribution of the frontier molecular orbitals (FMO).

Results: The results of the ETM-NN application to the series of compounds in view are pharmacophores and anti-pharmacophores, which are characteristic of the class of compounds demonstrating activity against *Mycobacterium tuberculosis* strain H37Rv. The statistical characteristics of five pharmacophores (Phi) and five anti-pharmacophores (APhi) entering the forecasting system, are 0.90 and 0.86, respectively. Molecular docking and electron density distribution analyzes revealed that the active compounds bind more strongly to the InhA enzyme.

Conclusion: A model of prognosis for the antitubercular activity of *Mycobacterium tuberculosis* H37Rv was developed on the base of the pharmacophores found, docking results, and electronic structure calculations. This model allows for designing of new potent antitubercular drugs.

Keywords: Tryptanthrin analogues, *Mycobacterium tuberculosis* H37Rv, InhA, electronic-topological method, molecular docking, density functional theory.

Öz

Amaç: Bu çalışmanın amacı, bir dizi triptantrın analogunun yapı-antitüberküloz aktivite ilişkilerini ve bu analogların *Mycobacterium tuberculosis* enoyl-acyl taşıyıcı protein (enoyl-ACP) redüktaz (InhA) ile bağlanma mekanizmalarını incelemektir.

Yöntem: İlk olarak, elektronik-topolojik yöntem (ETM) ile bileşiklerin yapısındaki farmakofor ve anti-farmakoforlar tespit edilmiş ve ETM-Sinir Ağları (*Neural Networks*, NN) yaklaşımına dayalı olarak aktivite tahmin modelleri geliştirilmiştir. İkinci aşamada, moleküler kenetlenme yöntemi kullanılarak bileşiklerin InhA enzimine bağlanma afiniteleri ve konformasyonları elde edilmiş; bağlanmada etkili olan kovalent olmayan etkileşimler incelenmiştir. Son aşamada, bu etkileşimler sınır moleküler orbitallerin (FMO) elektron yoğunluğu dağılımı üzerinden tartışılmıştır.

Bulgular: İnceleme altındaki bileşik serileri üzerine ETM-NN yönteminin uygulaması sonucunda *Mycobacterium tuberculosis* H37Rv suşuna karşı aktivite gösteren bileşiklerin karakteristik farmakofor ve anti-farmakofor özellik gösteren moleküler fragmanları tespit edilmiştir. Aktivite tahmin sistemine giren beş farmakofor (Phi) ve beş anti-farmakoforun (APhi) istatistiksel özellikleri sırasıyla 0,90 ve 0,86 olarak elde edilmiştir. Moleküler kenetlenme ve elektron yoğunluğu dağılımı analizleri, aktif bileşiklerin InhA enzimine daha kuvveti bağlandığını ortaya koymuştur.

Sonuç: Tespit edilen farmakofor gruplar, kenetlenme sonuçları ve elektronik yapı hesaplamalarına dayalı olarak, *Mycobacterium tuberculosis* H37Rv'nin antitüberküloz aktivitesi için bir prognoz modeli geliştirilmiştir. Bu prognoz modeli, yeni potansiyel antitüberküloz ilaçların tasarımında kullanılabilir.

Anahtar Kelimeler: Triptantrın analogları, *Mycobacterium tuberculosis* H37Rv, InhA, elektronik-topolojik yöntem, moleküler kenetlenme, yoğunluk fonksiyoneli teorisi.

* Corresponding author/İletişim kurulacak yazar: Fatma Aksakal; Department of Analytical Chemistry, Faculty of Pharmacy, Kocaeli Health and Technology University, Kocaeli, Türkiye

Phone/Telefon: +90 (262) 999 80 85 e-mail/e-posta: fatma.dagdelen@kocaelisaglik.edu.tr

Submitted/Başvuru: 01.02.2023

Accepted/Kabul: 15.02.2023

Published Online/ Online Yayın: 28.02.2023

Introduction

Tuberculosis (TB) is an infection arising from the bacillus *Mycobacterium tuberculosis* (*Mtb*). Globally in 2021, around 1.6 million people died from this infectious disease, of which 187000 were HIV co-infected.¹ Occurrence and spread of multidrug resistant tuberculosis (MDR-TB) along with extensively resistant tuberculosis (XDR-TB) make harder the problem, since few new medicines have been approved to fight the resistant forms.

Tryptanthrin (indolo[2,1-b] quinazoline-6,12-dione) is a compound from the class of tryptophan derived alkaloids produced by diverse plants²⁻⁵ and fungi.⁶ Tryptanthrin (TRYP) and its derivatives have been shown to induce a large number of biological effects in different *in vitro* and *in vivo* studies. These effects are antibacterial activity against *Bacillus subtilis*⁶, *Escherichia coli*⁷, MRSA⁸; antiprotozoal activity against *Leishmania donovani*⁹, *Plasmodium falciparum*^{10,11}, *Trypanosoma brucei*¹², *Toxoplasma gondii*^{13,14}; antifungal activity against *Malassezia furfur*⁸, *Trichophyton mentagrophytes*⁴; cytostatic or cytotoxic activity against MCF-7¹⁵⁻¹⁷, K-562¹⁸, NCI-H460, SF-268¹⁵, HeLa, SKOV-3¹⁷, WEHI-3B JCS¹⁹, U-937, HL-60²⁰ and A-498¹⁷ cell lines, and antiproliferative effects against tumor cells in Lewis lung cancer tumor-bearing mice¹⁷ and WEHI-3B JCS cells in syngeneic BALB/c mice.²¹

Interestingly, TRYP has been found to reduce resistance to some anticancer agents in breast cancer cells.^{16,17} One of the important activity of TRYPs is their following immunomodulatory effects: down-regulation of interleukin-4 production by Th2 cells¹⁹, inhibition of nitric oxide and prostaglandin E2 synthesis in macrophages²², inhibition of interferon- γ and interleukin-2 production by mouse spleen cells and Peyer's patch lymphocytes *in vitro*²³, indole amine 2,3-dioxygenase inhibition²⁴, significant decrease of the levels of TSLP, IL-4, IFN- γ , IL-6, TNF- α , chemokine, and caspase-1 in atopic dermatitis (AD), repression of the histidine decarboxylase levels with consequent reduction of histamine levels in AD.²⁵

TRYP and compounds derived from TRYP were proposed as immunotherapeutic agents to treat cancer, BCG, cholera, plague, typhoid, hepatitis B infection, influenza, inactivated polio, rabies, measles, mumps, rubella, oral polio, SARS, yellow fever, tetanus, diphtheria, Haemophilus influenzae type b, meningococcus and pneumococcus infections.^{26,27} Another reported activity of TRYP and its derivatives is antimycobacterial activity.^{28,29}

Enoyl-acyl carrier protein reductase (InhA) from *Mtb* is one of the key enzymes involved in the mycobacterium fatty acid biosynthetic pathway and is an effective antimicrobial target. InhA inhibitors are promising candidates for the development of novel antitubercular agents.³⁰

Molecular modelling and structure-activity relationships (SAR) studies play an essential role in the design of potential ligands that are both sterically and chemically compatible with the binding site of a target biomacromolecule.^{31,32} It should be noted that in literature there are a few computational works devoted to the ligand-receptor interaction for the enzyme InhA from *Mtb*.

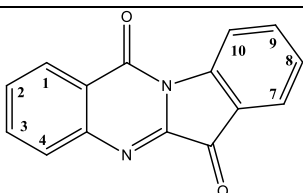
Novel antitubercular compounds identification through a hybrid virtual screening approach was investigated and molecular docking was performed to select the compounds on the base of their binding energies, binding modes, and tendencies to form reasonable interactions with InhA.³³ Effect of the explicit flexibility of the InhA enzyme from *Mtb* in molecular docking computations can be found in the literature.³⁴ The fully-flexible receptor models of InhA explicitly characterize the overall movements of the amino acid in helices, strands, loops and turns, allowing the ligand to properly accommodate itself in the receptor's binding site. Tripathi and coworkers³⁵ performed molecular docking analysis of TRYP and its analogues with InhA from *Mtb*. The study revealed that the alkaloid and its two analogues show a high affinity for the InhA binding site. Syntheses and docking of new modifications of the isoniazid-structure molecules are also presented in the literature.³⁶ *In silico* modeling on the InhA confirmed that longer alkyl substituents are advantageous for the molecular interactions and affinity to the enzyme. In one of the papers³⁷ on the inhibitors InhA from *Mtb*, docking of the compounds taken from the National Cancer Institute compound library against InhA was carried out. Analysing data on virtual screening, the authors described two promising and novel fragment hits that inhibit InhA activity.

In this study, molecular design of TRYP analogues and their interactions with InhA were reported. Firstly, structural and electronic factors influencing antitubercular activity of TRYP analogues were investigated. The structure-activity relationships study was performed using the electronic-topological method combined with Neural Networks (ETM-NN).^{38,39} Then, an antitubercular activity prediction model was improved to carry out computer screening of TRYP analogues. The prediction model was supported by the results of molecular docking and electronic structure computations of TRYP analogues in the active site of InhA enzyme.

Methods

Data set

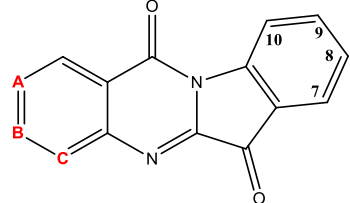
Initial data for the search of the structure-activity relationship is a learning series of compounds together with data on their activities.^{28,29} Molecular skeletons of the compounds are presented in Figure 1, while molecules with their substituents are given in Table 1.

Table 1. Compounds of the training and testing sets with different substituents


No	1	2	3	4	7	8	9	10	A/LA*
Training set									
1	H	H	H	H	H	H	H	H	A
2	H	Cl	H	H	H	F	H	H	A
3	H	H	H	H	H	Br	H	H	A
4	H	H	H	H	H	NO ₂	H	H	A
5	H	H	H	H	H	Cl	H	H	A
6	H	H	H	OCH ₃	H	F	H	H	A
7	H	H	F	H	H	F	H	H	A
8	H	H	H	H	H	CO ₂ Et	H	H	A
9	H	H	H	H	H	H	F	H	LA
10	H	H	H	OCH ₃	H	I	H	H	A
11	H	I	H	I	H	CO ₂ Et	H	H	LA
12	H	H	F	H	H	Cl	H	CH ₃	A
13	H	F	NBP	H	H	I	H	H	LA
14	F	Br	H	Br	H	I	H	H	A
15	F	Br	H	Br	H	H	H	H	LA
16	H	F	3-MNBP	H	H	I	H	H	LA
17	H	H	H	OCH ₃	H	CO ₂ Et	H	H	A
18	H	H	H	OCH ₃	H	SO ₂ n-octyl	H	H	LA
19	H	H	H	OCH ₃	H	SO ₂ NMP	H	H	LA
20	H	H	H	OCH ₃	H	CO ₂ H	H	H	LA
21	H	NO ₂	H	H	H	H	H	H	LA
22	Cl	H	Cl	H	H	H	H	H	LA
23	H	H	H	H	H	NH ₂	H	H	LA
24	H	F	3-MP	H	H	CO ₂ H	H	H	LA
25	H	OPO ₃ Na ₂	H	H	H	H	H	H	LA
26	H	OH	H	H	H	H	H	H	LA
27	H	octyl	H	H	H	H	H	H	LA
28	H	6-acocetenyl	H	H	H	Cl	H	H	LA
29	H	H	H	H	H	Cl	Pip	H	LA
30	H	H	H	H	H	CF ₃	H	H	A
31	H	H	F	H	H	OCF ₃	H	H	A
32	H	F	H	H	H	Cl	H	H	A
33	H	H	H	H	H	OCF ₃	H	H	A
Test set									
34	H	H	H	H	H	F	H	H	A
35	H	H	H	OBn	H	F	H	H	LA
36	H	H	H	H	H	I	H	H	A
37	H	F	H	H	H	F	H	H	A
38	H	Br	H	H	H	F	H	H	A
39	H	CH ₃	H	CH ₃	H	F	H	H	A
40	H	CH ₃	H	H	H	H	H	H	LA
41	H	I	H	I	H	I	H	H	LA
42	H	2-AG	H	H	H	Cl	H	H	LA
43	H	H	octyl	H	H	octyl	H	H	LA

The compounds are the TRYP analogues possessing high and middle level of antitubercular activity. As seen from Figure 1, the molecules differ from each other by their substituents in the rings they contain. To adjust to the series more representative, it was added a few active heterocyclic compounds (III-X) with structures that are quite different from the structure of TRYP.

The search for pharmacophores responsible for the compounds, bioactivity was carried out in two groups of compounds taken from the initial series. In one of them there were highly active compounds (43 molecule, MIC < 0.125 µg/ml), and the other included low-active compounds (29 molecules, MIC > 4 µg/ml). Besides, training set (63 molecules, including III-X) and test set (17 molecules) were formed to evaluate the effectiveness of the activity/inactivity fragments found.

Table 1. Continued


No	A	B	C	7	8	9	10	A/LA*
Training set								
44	CH	CH	N	H	Br	H	H	A
45	CH	CH	N	H	Cl	H	H	A
46	CH	CH	N	H	F	F	H	LA
47	CH	CH	N	H	I	H	H	A
48	CH	CH	N	H	CO ₂ Et	H	H	A
49	N	CH	CH	H	I	H	H	A
50	N	CH	CH	H	Cl	H	H	A
51	N	CH	CH	H	Br	H	H	A
52	N	CH	CH	H	1-octenyl	H	H	A
53	N	CH	CH	H	n-octyl	H	H	A
54	CH	CH	N	CF ₃	I	H	H	A
55	N	CH	CH	H	CF ₃	H	H	A
56	CH	CH	N	CF ₃	Cl	H	H	A
57	N	CH	CH	H	OCF ₃	H	H	A
58	N	CH	CH	H	n-butyl	H	H	A
59	N	CH	CH	H	CH(i-propyl)OCH ₃	H	H	A
60	CH	N	CH	H	OCF ₃	H	H	A
61	N	H	H	H	H	Pip	H	LA
62	N	H	H	H	H	Mor	H	LA
63	N	H	H	H	H	Prz	H	LA
64	H	H	N	H	H	Pip	H	LA
65	H	H	N	H	H	H	H	LA
Test set								
66	N	CH	CH	H	SO ₂ CH ₃	H	H	LA
67	N	CH	CH	H	1-hexyl	H	H	A
68	N	CH	CH	H	DMDOx	H	H	A
69	N	CH	CH	H	MH	H	H	A
70	N	CH	CH	H	cyclohexyl	H	H	A
71	N	CH	CH	H	2-octyl	H	H	A
72	CH	CH	N	H	OCF ₃	H	H	A

*A: highly active, LA: low-active; 2-AG: 2-(acetoxymethyl)-6-(allyloxy)tetrahydro-2H-pyran-3,4,5-triyl triacetate; NBP: 3-n-butylphthalide; NMP: N-Methyl-2-pyrrolidone; 3-MNBP:3-methyl-3-n-butylphthalide; DMDOx: 2-(5,5-dimethyl-1,3-dioxanyl); MH: 3-(2-methylheptyl); 3-MP: 3-methyl-2-pyrrolidinone; Pip: piperidine; Bn: benzyl; Mor: morpholine; Prz: piperaziny.

Description of Electronic-Topological Method (ETM)

Since ETM is explained in detail in the literature,³⁹⁻⁴⁶ the most distinctive features of ETM compared to other structure-activity relationship approaches are given in this section. ETM belongs to the so-called structural methods. So, the base for the method is a language for the compounds' structure description. This language reflects the discrete nature of molecules as groups of atoms, some of which are chemically bonded. Labeled graphs appeared to be the most appropriate mathematical counterparts for chemical structures together with relationships on their atoms and bonds. The representative of a graph is a matrix of order $n \times n$; where n is the number of vertices of the graph. Therefore, ETM proposes Electronic-Topological Matrices of Contiguity (ETMC) for the identification of chemical compounds. Bonds have no direction, so matrices are symmetric with respect to their left diagonal, and it is sufficient to have only the upper right triangle of any such matrix with its diagonal.

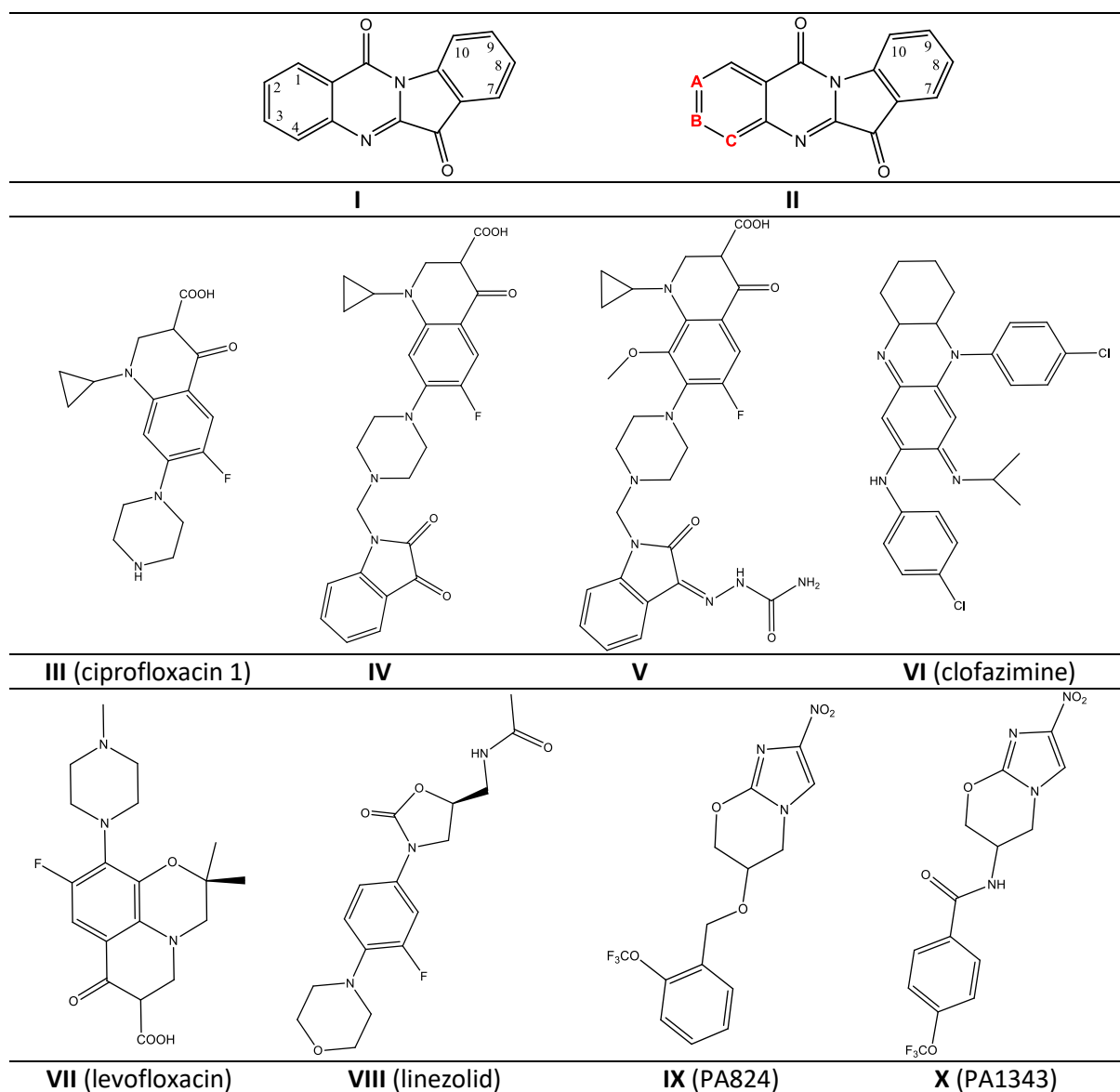


Figure 1. Structures of tryptanthrin (I), its analogues (II) and some antitubercular drugs (III-X)

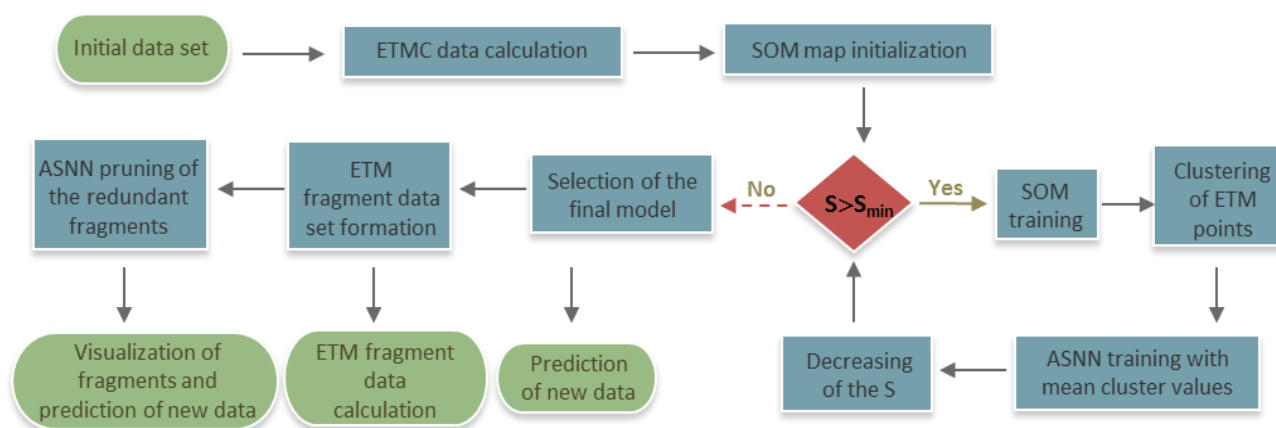


Figure 2. Block-scheme of data analysis with ETM-NN.

Vertices of such graphs (diagonal elements a_{ii} of the ETMCs) are naturally labeled by values representing atomic characteristics (charges- q_i , frontier molecular orbital coefficients *etc.*). For off-diagonal elements there are two possibilities. If they represent chemical bonds, then one of the bond characteristic is to be chosen for all matrices and fixed (here, Wiberg's indices, W_{ij}). Otherwise, the corresponding distance value is taken for the given pair of atoms (R_{ij}).

For a selected activity, the goal of the ETM approach is to identify molecular fragments common to all active compounds (pharmacophores, Ph) and not found in all inactive compounds (anti-pharmacophores, APh) with similar structures. A number of fragments characterizing inactive compounds will likewise be found. The pharmacophores and the anti-pharmacophore set are essential molecular substructures that provide a model for the prediction of the activity in view. This model can be used both for testing newly synthesized compounds, and for the computer modeling of new candidates for the purposeful syntheses.

To automate the activity estimation procedure, ETM application is followed by an associative neural networks (ASNNs) application (with unsupervised and supervised learning algorithms), and this approach is named as ETM-NN.³⁸ The ANNs application uses data of the ETM computations being electronic-topological submatrices of contiguity (ETSC) for Ph and APh as input for a new algorithm developed on the base of Volume Learning Algorithm. It had been used previously for the CoMFA analysis.^{47,48} This algorithm is implemented as a recurrent iterative application of the Kohonen self-organizing maps (SOMs) and ASNNs.^{49,50}

The later version of ETM using neural networks (ETM-NN) for data optimization and features extraction is working with the structures of compounds optimized through their interaction with receptor (in the process of the ETMCs formation), *i.e.* with the structures that are mostly profitable for the interaction with receptor conformations. This helped to solve the problem of finding the proper initial conformation for flexible molecules (flexibility problem). Conformational analysis and the electronic properties study are carried out for all compounds by using Gaussian 09 program.⁵¹ General block-scheme of ETM-NN is given in Figure 2.

The first step is to prepare an initial data set for the SOM algorithm training (triples computation). The data sample is a triple ($d1$, $d2$, $d3$), where $d1$ and $d2$ are charges of two atoms and $d3$ is a connection between them. The d_i values, $i=1, 2, 3$ are taken from the ETMCs. The total number of data samples corresponds to the amount of all two-atom connections taken from all ETMCs.

The second step includes initialization and training of the Kohonen's network of the size $S=x*y$. The initial size of Kohonen's maps was $S=2*S_{ETM}$, with S_{ETM} being the size of the largest ETM matrix. Upon subsequent compressions, the map size was decreased by two units in both x and y directions. When using the Kohonen's networks, it is possible to create a nonlinear projection of high-dimensional data set onto a low-dimensional domain. To train a Kohonen's map, two phases are needed. The first phase of 50,000 iterations is used for the weight vectors of the map neurons rough ordering. During the second phase (100,000 iterations), the values of the weight vectors are fine-tuned. The initial learning rate and neighborhood radius of the SOM under training are selected to be $\alpha_1=0.6$, $\sigma_1=2/5(x*y)^{0.5}$ and $\alpha_2=0.15$, $\sigma_2=2/5\sigma_1$ for the first and the second phase, respectively. To form a compressed sample data set, the cluster

centers (C_n) were calculated by averaging over all values entering into the given cluster, $C_n = Xn_i/m$, where Xn_i was the value of the i -th element of the ETMC for the n -th molecule, and m was the number of ETMC values entering into the cluster for the molecule n .

At the third step, the compressed data are tested on the three-layer ASNNs. From the mean values of input parameters for each cluster, a new data set is formed for the ASNN learning. The number of neurons in the input layer corresponds to the number of clusters obtained as the output of the SOM. The hidden layer contains five neurons. The bias neuron is presented both on the input and hidden layer. An ensemble of $M=100$ neural networks was trained. The activity values were calculated for each network (ASNN) and averaged over all M networks. This value was used to calculate the statistical coefficients. The quality of each final model was assessed by the leave-one-out (LOO) method. By the method, each molecule is removed from the training set, and the remaining set is used to separate molecules into classes of activity, thereby predicting the activity of this molecule and evaluating the quality of the decision rule.

The fourth step is the computation of pharmacophores as the ETMCs fragments. At the fifth step, the weight of each fragment is estimated for each compound as its projection error, E_q , relative to the same nodes of the Kohonen's map as its comprising ETMC. The weight is taken as the inverse of its E_q : $W_{ij}=1/E_{qij}$ (i : molecule's number, j : fragment's number). A new table is formed based on the weight coefficients computed using the fragment weights as parameters.

In the final step, pruning algorithms targeting the selection of the most relevant ETMC fragments are applied. Optimized fragments, found to be important for displaying the activity analyzed by the molecules, are used to visualize these regions of the molecules under study.

Molecular docking computations

In order to gain insight into the binding mode of compounds to InhA and make interpretation of the obtained results, molecular docking was carried out. 3D-crystallographic structure of the target enzyme InhA was retrieved through RCSB Protein Data Bank (<http://www.rcsb.org/pdb/>), under the accession code 4U0J.³⁰ Before the molecular docking, the geometry of initial structures has been built and optimized by using the Gaussian 09 program. All these structures were calculated by using Density Functional Theory (DFT) at the B3LYP (Becke, three-parameter, Lee-Yang-Parr)/6-31G(d,p) level.^{52,53}

For the docking studies, MOE⁵⁴ software was used to estimate free energies of the enzyme-ligand binding. The enzyme-ligand complexes were minimized up to a gradient of 0.01 kcal/(mol Å), and hydrogens were added using the force field AMBER99. Charges on the protein were assigned using the force field AMBER99, while the charges on the ligands were assigned by using force field MMF94X. The docked poses for the compounds under

study were scored using London ΔG scoring function for finding the best docking pose.

Results

Analysis of pharmacophores and anti-pharmacophores

The ETM application made it possible to reveal in the two groups both molecular fragments characterizing the presence of activity (pharmacophores) and fragments inhibiting the activity (anti-pharmacophores). A pharmacophore (Ph) is represented by a submatrix of an ETMC, which isomorphically enters the structures of all active compounds. Its realization in this class can be assessed by a P_a parameter, which characterizes effectiveness of the pharmacophore. The closer its value to the unit, the more guaranty that a compound belongs to the class of active molecules. Analogous estimates can be calculated for the class of low-active compounds when searching for the anti-pharmacophoric molecular fragments.

In the matrix comparison stage (testing whether atoms and bonds match) the optimum values of variations allowed were found as $\Delta_1 = \pm 0.07$ for diagonal elements (q_i) and $\Delta_2 = \pm 0.20$ for off-diagonal values (W_{ij} and R_{ij}). The lowest level of probabilistic estimates, P_a , was taken as 0.80 to determine the most informative activity features. To form the basis of a model for the antitubercular activity prediction, compound **57** possessing the highest activity was taken first of all as a template for the comparison. In Fig. 3a, a submatrix of this template ETMC (ETSC) is given, which corresponds to one of pharmacophores revealed (Ph1).

As seen, Ph1 consists of negatively charged atoms attached to the A and D rings. Their charges are changing in the range between -0.01 e and -0.20 e , and maximum distance between the atoms belonging to the fragment is 10.36 \AA (N2.....O20) (Figure 3a). The other pharmacophore, Ph2, includes 7 atoms that are negatively charged as well. Maximal value of distance equals 11.15 \AA (C2.....O22). Ph2 (template compound **8**) is characterized by the presence of atoms belonging to the cycles A, B and by the oxygen atom of the $-\text{CO}_2\text{Et}$ group, attached to the cycle D (Figure 3b). The probabilities of Ph1 and Ph2 realization, *i.e.* P_a values, are 0.94 and 0.92, respectively.

Analysis of the APh1 and APh2 anti-pharmacophores (corresponding to template compounds **20** and **25**) has shown that they differ from Ph1 and Ph2 in the part of charge distribution on the atoms and by their spatial topology as well (Figure 4).

While the class of active compounds is characterized by the presence of a nitrogen in the cycle A, then the class of low-active compounds is represented by the phenyl cycle with varying substituents.

In Table 2, some of the pharmacophores (Phi) and anti-pharmacophores (APhi) are given, which have been found for different template molecules. All data are given both for training set and for the test set of molecules. As

seen from Table 2, the values of P_a vary in the limits of 0.87–0.94 and 0.82–0.90 for pharmacophores and anti-pharmacophores, respectively.

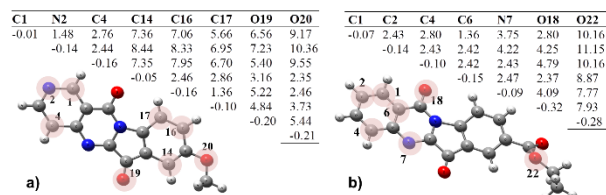


Figure 3. Two pharmacophores, Ph1 and Ph2, found relative to corresponding active templates **57** (a) and **8** (b)

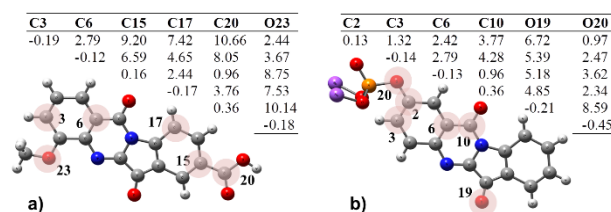


Figure 4. Two anti-pharmacophores, APh1 and APh2, found relative to corresponding inactive templates **20** (a) and **25** (b)

Table 2. Statistical characteristics for some of pharmacophores (Phi) and anti-pharmacophores (APhi) calculated by ETM

Phi (template compound)	P_a	P_{ia}	APhi (template compound)	P_a	P_{ia}
Ph1 (57)	0.94	0.06	APh1 (20)	0.10	0.90
Ph2 (8)	0.92	0.08	APh2 (25)	0.11	0.89
Ph3 (5)	0.90	0.10	APh3 (12)	0.14	0.86
Ph4 (44)	0.88	0.12	APh4 (23)	0.16	0.84
Ph5 (54)	0.87	0.13	APh5 (29)	0.18	0.82
Average	0.89	0.11	Average	0.15	0.85

Application of ETM-NN Approach

The first stage of the ETM-NN data analysis was to find a cluster distribution model capable of reflecting the realistic internal structure of the data; and its results are given in Table 3.

For the training set, 54 clusters were found. ASNNs recognized correctly 92% (58 from 63 compounds), while for the test set the predictive ability was a bit lower, namely, 88% (15 compounds from 17). For the summary set, the result was 90% (73 compounds from 80). These results tell in favor of high quality of the cluster distribution model and its fitness for the analysis of new data sets, *i.e.* for the search for pharmacophores.

At the second stage, only 25 fragments were selected for the training and test sets (Table 4). On the base of the weights calculated for the molecular fragments represented by ETSCs, ASNN were capable of recognizing 95% (60 compounds from 63) in the training set, and 88% (15 compounds from 17) in the test set. In total, the network classified correctly 94%, or 75 compounds from 80.

Table 3. Cross-validated q^2 coefficients calculated for Tryptanthrin analogues.

Data set	All pharmacophores		
	WD _s * number	Molecule Amount	Molecule Predicted (P _a)
Training set	54	63	58 (0.92)
Test set	54	17	14 (0.86)
Total	54	80	72 (0.90)

* WD_s: weight descriptors**Table 4.** Cross-validated q^2 coefficients calculated for Tryptanthrin analogues on the base of fragment data set.

		Param.	Molecule	
		number	Amount	Predicted (%)
All Ph*	Training set	25	63	60 (95)
	Test set	25	17	15 (88)
	Total	25	80	75 (94)
Ph selected by pruning methods	Training set	20	63	59 (94)
	Test set	20	17	15 (88)
	Total	20	80	74 (93)

*Ph: Pharmacophores

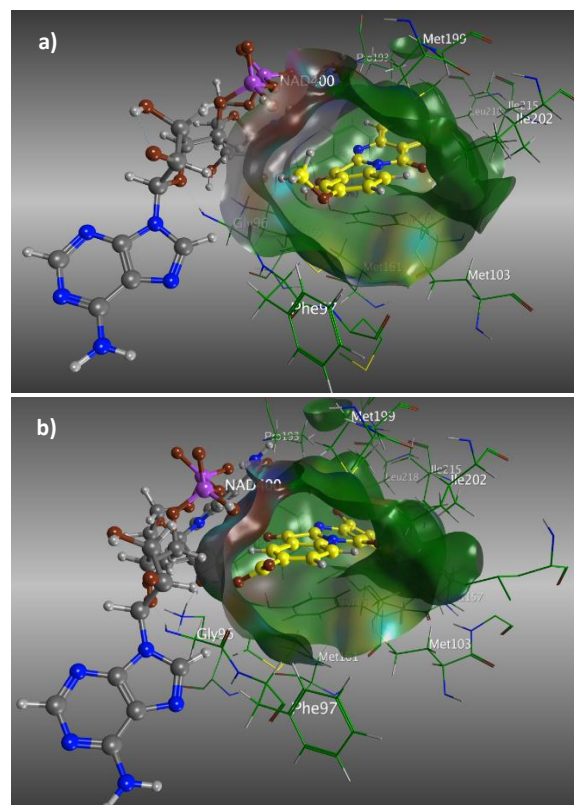
The pruning methods application afforded to select only 20 of them as the most influential fragments. By this, ASNN classified correctly 94%, that is 59 compounds from 63 in the training set, and 88%, or 15 compounds from 17, in the test set. In the summary set, ASNNs classified correctly 93% (74 compounds from 80).

In our case, comparison of two models (one model based on the cluster distribution found in a straightforward manner, and another based on training the network by the ETMCs for fragments) tells in favor of close correspondence between their results. However, the first model is not stable enough and depends severely on the structures of compounds selected for the training set. However, in comparison with other commonly used approaches, the approach presented in this study has shown quite satisfactory results, which tell about workability of both models found, and both can be applied for the design of new potent antitubercular drugs.

Based on the pharmacophores and anti-pharmacophores found, the model for the antitubercular activity prediction had been successfully applied to the activity estimation in a series of Tryptanthrin analogues. However, molecular docking and frontier molecular orbital (highest occupied molecular orbital, HOMO and lowest unoccupied molecular orbital, LUMO) analyses were performed for these compounds to understand the mechanism of their actions in detail.

Molecular docking results

In the framework of the ETM-NN study, docking of template compounds into the active site of InhA has been carried out. The best docking poses of active compound **57** and inactive compound **20** in the active site of InhA were represented in Figure 5.

**Figure 5.** 3D representation of docked poses of compounds **57** (a) and **20** (b) in the active site of InhA (PDB code: 4U0J)

Close interaction with such amino acids as Tyr158, Phe149, Met161, Ile215, Gly96, and Met199 is observed in the case of template compound **57**. As to low-active compound **20**, amino acids Gly96, Tyr158, Phe149, and Met199 are involved into the interaction. It should be stressed that there exists a noticeable difference in the energy of binding with receptor in the two cases. For the active compound **57** it is $-15.5 \text{ kcal mol}^{-1}$, for the low-active **20** it equals to $-7.3 \text{ kcal mol}^{-1}$. Analogous situation is observed for the other pair of template compounds, **8** and **25**. The energy of binding with receptor is considerably higher for the high-active molecule **8** than for the low-active molecule **25** (-16.1 and $-10.8 \text{ kcal mol}^{-1}$, respectively).

Frontier Molecular Orbital (FMO) analyses

The analysis of specificity of the enzyme-ligand interaction is closely related to the analysis of frontier orbitals (HOMO and LUMO) in molecular systems. The electron density distribution on the frontier orbitals of the enzyme-ligand complexes under study tells about donor-acceptor character of the interaction inside the complexes. The electronic structure computations were carried out with the Gaussian 09 using DFT at the B3LYP/6-31G(d,p) level. 3D structures of ligand and active site of enzyme were taken from the molecular docking.

When active compounds bind with InhA, atoms of amino acid residues and atoms of ligands form the frontier orbitals of the formers. For the low-active compounds, the character of the electron density distribution is a bit

different. As an example, Fig. 6 shows the electron density distribution on the frontier orbitals formed by the active sites of InhA with active compound **57** (Figure 6a and 6b) and low active compound **20** (Figure 6c and 6d). It is worth to be noted that the electron density

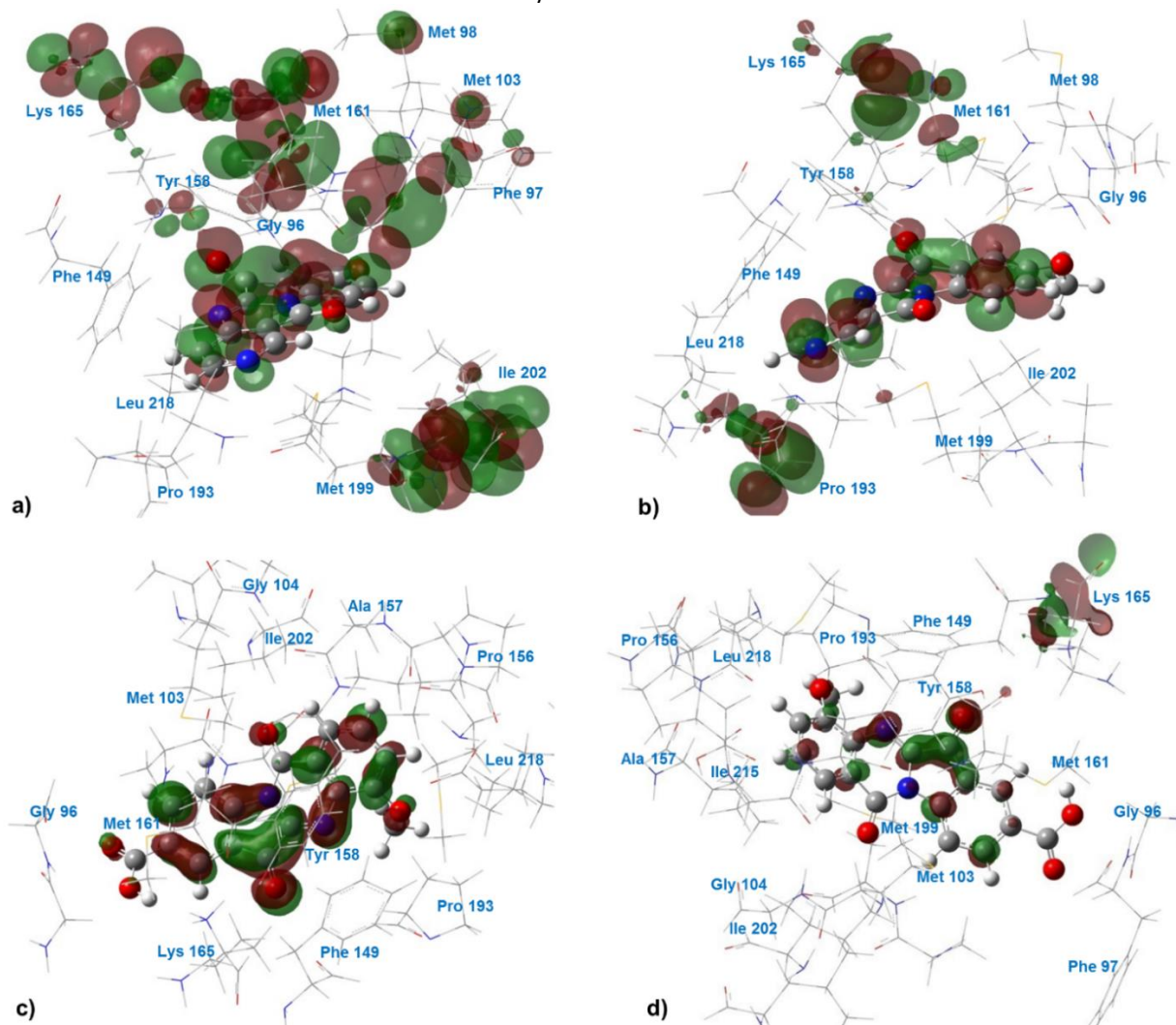


Figure 6. 3D view of HOMO (a, c) and LUMO (b, d) for the active site of InhA with active compound **57** (a, b) and inactive compound **20** (c, d)

In addition, HOMO is formed by the atoms of both **57** and amino acids of the InhA active site (Lys165, Met161, Gly96, Phe97, Ile202, Met199, Leu218) (Figure 6a). As to the LUMO, the electron density is concentrated on the atoms of ligand and those of amino acids Met161 and Pro193 (Figure 6b).

For the template low-active compound **20** and InhA complex, electron density is distributed mainly on the atoms of the ligand (Figure 6c and 6d). Moreover, the role of frontier orbitals in the ligand-receptor interaction is not significant. The analysis of the electron distribution in two groups of compounds (active and low active ones) shows that it is the frontier orbitals' nature in the ligand-receptor complexes within active site of InhA that plays very important role for the antitubercular activity prediction in the series of tryptanthrin analogues. Both groups enter the system of the activity prediction.

distribution on the frontier orbitals of InhA-**57** complex is such that donor-acceptor interaction is specific for the HOMO, while low acceptor interaction is characteristic of the LUMO.

Conclusion

A series of Tryptanthrin analogues were studied with the aim of finding peculiarities of conformational and electronic structures of compounds. The researches were carried out for structurally diverse set of 80 molecules. The results of the ETM-NN application to the series of compounds in view are pharmacophoric and anti-pharmacophoric molecular fragments, which are characteristic of the class of compounds demonstrating activity against *Mtb* H37Rv. The statistical characteristics of five pharmacophores (Ph_i) and five anti-pharmacophores (APh_i) entering the forecasting system, are 0.90 and 0.86, respectively. The fragments selected serve as a base for the further prognosis and design of antitubercular molecules.

Analysis of the molecular docking and electron density distribution has shown that the more effective binding

with receptor was observed for active compounds. A model of prognosis for the antitubercular activity of *Mtb* H37Rv was developed on the base of the pharmacophores found, docking results, and electronic structure computations. This prognosis model allows for carrying out screening and design of new potent antitubercular drugs.

Acknowledgements

I would like to thank Prof. Anatoli Dimoglo, who is one of the developers of the ETM and ETM/NN methods I have used in this study, for his valuable contribution to the implementation of these methods.

Ethical Approval

No ethics committee decision is required for the study.

Financial Disclosure

None.

References

1. Bagcchi S. WHO's Global Tuberculosis Report 2022. *The Lancet Microbe*. 2023;4(1):e20. doi:10.1016/S2666-5247(22)00359-7
2. Bergman J, Lindström J-O, Tilstam U. The structure and properties of some indolic constituents in *Couroupita guianensis* aubl. *Tetrahedron*. 1985;41(14):2879-2881. doi: 10.1016/S0040-4020(01)96609-8
3. Honda G, Tabata M. Isolation of antifungal principle tryptanthrin, from *Strobilanthes cusia* O. Kuntze. *Planta medica*. 1979;36(1):85. doi: 10.1016/S0040-4020(01)96609-8
4. Honda G, Tosirisuk V, Tabata M. Isolation of an antidermatophytic, tryptanthrin, from indigo plants, *Polygonum tinctorium* and *Isatis tinctoria*. *Planta medica*. 1980;38(3):275-276. doi: 10.1055/s-2008-1074877
5. George V, Koshy A, Singh O, et al. Pushpangadan P. Tryptanthrin from *Wrightia tinctoria*. *Fitoterapia*. 1996;67(6):553-554.
6. Schindler F, Zähner H. Stoffwechselprodukte von Mikroorganismen. *Archiv für Mikrobiologie*. 1971;79(3):187-203. doi: 10.1007/BF00408783
7. Bandekar PP, Roopnarine KA, Parekh VJ, et al. Antimicrobial activity of tryptanthrins in *Escherichia coli*. *Journal of medicinal chemistry*. 2010;53(9):3558-3565. doi: 10.1021/jm901847f
8. Kawakami J, Matsushima N, Ogawa Y, et al. Antibacterial and antifungal activities of tryptanthrin derivatives. *Transactions of the Materials Research Society of Japan*. 2011;36(4):603-606. doi: 10.14723/tmrj.36.603
9. Bhattacharjee AK, Skanchoy DJ, Jennings B, et al. Analysis of stereoelectronic properties, mechanism of action and pharmacophore of synthetic indolo [2, 1-b] quinazoline-6, 12-dione derivatives in relation to antileishmanial activity using quantum chemical, cyclic voltammetry and 3-D-QSAR CATALYST procedures. *Bioorganic & medicinal chemistry*. 2002;10(6):1979-1989. doi: 10.1016/s0968-0896(02)00013-5
10. Bhattacharjee AK, Hartell MG, Nichols DA, et al. Structure-activity relationship study of antimalarial indolo [2, 1-b] quinazoline-6, 12-diones (tryptanthrins). Three dimensional pharmacophore modeling and identification of new antimalarial candidates. *European journal of medicinal chemistry*. 2004;39(1):59-67 doi:10.1016/j.ejmech.2003.10.004
11. Onambele LA, Riepl H, Fischer R, et al. Synthesis and evaluation of the antiplasmodial activity of tryptanthrin derivatives. *International Journal for Parasitology: Drugs and Drug Resistance*. 2015;5(2):48-57. doi: 10.1016/j.ijpddr.2015.03.002
12. Scovill J, Blank E, Konnick M, et al. Antitrypanosomal activities of tryptanthrins. *Antimicrobial agents and chemotherapy*. 2002;46(3):882-883. doi: 10.1128/AAC.46.3.882-883.2002
13. Krivogorsky B, Grundt P, Yolken R, et al. Inhibition of *Toxoplasma gondii* by indirubin and tryptanthrin analogs. *Antimicrobial agents and chemotherapy*. 2008;52(12):4466-4469. doi: 10.1128/AAC.00903-08
14. Krivogorsky B, Nelson AC, Douglas KA, et al. Tryptanthrin derivatives as *Toxoplasma gondii* inhibitors—structure–activity-relationship of the 6-position. *Bioorganic & medicinal chemistry letters*. 2013;23(4):1032-1035. doi: 10.1016/j.bmcl.2012.12.024
15. Jao C-W, Lin W-C, Wu Y-T, et al. Isolation, structure elucidation, and synthesis of cytotoxic tryptanthrin analogues from *Phaius mishmensis*. *Journal of natural products*. 2008;71(7):1275-1279. doi: 10.1021/np800064w
16. Yu S-T, Chen T-M, Tseng S-Y, et al. Tryptanthrin inhibits MDR1 and reverses doxorubicin resistance in breast cancer cells. *Biochemical and biophysical research communications*. 2007;358(1):79-84. doi: 10.1016/j.bbrc.2007.04.107
17. Yu S-t, Chern J-w, Chen T-m, et al. Cytotoxicity and reversal of multidrug resistance by tryptanthrin-derived indoloquinazolines. *Acta Pharmacologica Sinica*. 2010;31(2):259-264. doi: 10.1038/aps.2009.198
18. Miao S, Shi X, Zhang H, et al. Proliferation-attenuating and apoptosis-inducing effects of tryptanthrin on human chronic myeloid leukemia K562 cell line in vitro. *International journal of molecular sciences*. 2011;12(6):3831-3845. doi: 10.3390/ijms12063831
19. Iwaki K, Ohashi E, Arai N, et al. Tryptanthrin inhibits Th2 development, and IgE-mediated degranulation and IL-4 production by rat basophilic leukemia RBL-2H3 cells. *Journal of ethnopharmacology*. 2011;134(2):450-459. doi: 10.1016/j.jep.2010.12.041
20. Kimoto T, Hino K, Koya-Miyata S, et al. Cell differentiation and apoptosis of monocytic and promyelocytic leukemia cells (U-937 and HL-60) by tryptanthrin, an active ingredient of *Polygonum tinctorium* Lour. *Pathology international*. 2001;51(5):315-325. doi: 10.1046/j.1440-1827.2001.01204.x
21. Chan H-L, Yip H-Y, Mak N-K, et al. Modulatory effects and action mechanisms of tryptanthrin on murine myeloid leukemia cells. *Cellular and Molecular Immunology*. 2009;6(5):335. doi: 10.1038/cmi.2009.44
22. Ishihara T, Kohno K, Ushio S, et al. Tryptanthrin inhibits nitric oxide and prostaglandin E(2) synthesis by murine macrophages. *European journal of pharmacology*. 2000;407(1):197-204. doi: 10.1016/s0014-2999(00)00674-9
23. Takei Y, Kunikata T, Aga M, et al. Tryptanthrin inhibits interferon-gamma production by Peyer's patch lymphocytes derived from mice that had been orally administered staphylococcal enterotoxin. *Biological and Pharmaceutical Bulletin*. 2003;26(3):365-367. doi: 10.1248/bpb.26.365

24. Yang S, Li X, Hu F, et al. Discovery of tryptanthrin derivatives as potent inhibitors of indoleamine 2, 3-dioxygenase with therapeutic activity in Lewis lung cancer (LLC) tumor-bearing mice. *Journal of medicinal chemistry*. 2013;56(21):8321-8331. doi: 10.1021/jm401195n
25. Han N-R, Moon P-D, Kim H-M, et al. Tryptanthrin ameliorates atopic dermatitis through down-regulation of TSLP. *Archives of biochemistry and biophysics*. 2014;542:14-20. doi: 10.1016/j.abb.2013.11.010
26. Valiante NM. Administering a tryptanthrin compound, eg, 8-nitroindolo[2,1-b]quinazoline-6,12-dione, to potentiate the immune response to an antigen; immunostimulants; small molecule immune potentiators; immunotherapy for infectious diseases; anticarcinogenic agents; vaccine adjuvant compositions and kits. *Google Patents*; 2012.
27. Jahng Y. Progress in the studies on tryptanthrin, an alkaloid of history. *Archives of pharmacal research*. 2013;36(5):517-535. doi: 10.1007/s12272-013-0091-9
28. Baker WR, Mitscher LA. Indolo[2,1-b]quinazoline-6,12-dione antibacterial compounds and methods of use there of. U.S. Patent No. 5,441,955. Washington, DC: U.S. *Patent and Trademark Office*. 1995.
29. Mitscher LA, Baker W. Tuberculosis: a search for novel therapy starting with natural products. *Medicinal research reviews*. 1998;18(6):363-374. doi: 10.1002/(SICI)1098-1128(199811)18:6<363::AID-MED1>3.0.CO;2-I
30. He X, Alian A, Stroud R, et al. Pyrrolidine carboxamides as a novel class of inhibitors of enoyl acyl carrier protein reductase from *Mycobacterium tuberculosis*. *Journal of medicinal chemistry*. 2006;49(21):6308-6323. doi: 10.1021/jm060715y
31. Karunakaran S, Subhashchandrabose S, Lee KW, et al. Investigation on the isoform selectivity of novel kinesin-like protein 1 (KIF11) inhibitor using chemical feature based pharmacophore, molecular docking, and quantum mechanical studies. *Computational Biology and Chemistry*. 2016; 61:47-61. doi: 10.1016/j.compbiolchem.2016.01.002
32. Turabekova MA, Rasulev BF, Levkovich MG, et al. Aconitum and Delphinium sp. alkaloids as antagonist modulators of voltage-gated Na⁺ channels: AM1/DFT electronic structure investigations and QSAR studies. *Computational biology and chemistry*. 2008;32(2):88-101. doi:10.1016/j.compbiolchem.2007.10.003
33. Muddassar M, Jang JW, Gon HS, et al. Identification of novel antitubercular compounds through hybrid virtual screening approach. *Bioorganic & medicinal chemistry*. 2010;18(18):6914-6921. doi: 10.1016/j.bmc.2010.07.010
34. Cohen EM, Machado KS, Cohen M, et al. Effect of the explicit flexibility of the InhA enzyme from *Mycobacterium tuberculosis* in molecular docking simulations. *BMC genomics*. 2011;12(Suppl 4):S7.
35. Tripathi A, Wadia N, Bindal D, et al. Docking studies on novel alkaloid tryptanthrin and its analogues against enoyl-acyl carrier protein reductase (InhA) of *Mycobacterium tuberculosis*. *Indian J Biochem Biophys*. 2012;49(6):435-41.
36. Rychtarčíková Z, Krátký M, Gazvoda M, et al. N-Substituted 2-Isonicotinoylhydrazinecarboxamides—New antimycobacterial active molecules. *Molecules*. 2014;19(4):3851-3868. doi:10.3390/molecules19043851
37. Perryman AL, Yu W, Wang X, et al. A virtual screen discovers novel, fragment-sized inhibitors of *Mycobacterium tuberculosis* InhA. *Journal of chemical information and modeling*. 2015;55(3):645-659. doi: 10.1021/ci500672v
38. Dimoglo A, Kovalishyn V, Shvets N, et al. The structure-inhibitory activity relationships study in a series of cyclooxygenase-2 inhibitors: A combined Electronic-Topological and Neural Networks Approach. *Mini Reviews in Medicinal Chemistry*. 2005;5(10):879-892. doi:10.2174/138955705774329537
39. Dimoglo AS. Compositional approach to electronic structure description of chemical compounds, oriented on computer analysis of structure-activity relationships. *Khimiko-Pharmazevticheskii Zhurnal*. 1985;4:438-444.
40. Dimoglo AS. In: Saley L, ed. Coordinational and organic biologically active compounds. *Stiinta*; 1986:7-11.
41. Shvets N. Applied program system for the prognosis of biological activity of chemical compounds: Development and use. *Computer Journal of Moldova*. 1993;3:101-110.
42. Shvets NM, Dimoglo A. Structure-odor relationships: results of an applied electron-topological approach. *Nahrung*. 1998;42(6):364-370. doi: 10.1002/(sici)1521-3803(199812)42:06<364::aid-food364>3.3.co;2-e
43. Oruç EE, Rollas S, Kandemirli F, et al. 1,3,4-thiadiazole derivatives. Synthesis, structure elucidation, and structure-antituberculosis activity relationship investigation. *Journal of Medicinal Chemistry*. 2004/12/01 2004;47(27):6760-6767. doi:10.1021/jm0495632
44. Bersuker IB, Dimoglo AS. The Electron-Topological Approach to the QSAR problem. In: Lipkowitz KB, Boyd DB, eds. *Reviews in Computational Chemistry*. John Wiley & Sons, Inc.; 2007:423-460. doi: 10.1002/9780470125793.ch10
45. Karalı N, Gürsoy A, Kandemirli F, et al. Synthesis and structure-antituberculosis activity relationship of 1H-indole-2,3-dione derivatives. *Bioorganic & Medicinal Chemistry*. 9/1/ 2007;15(17):5888-5904. doi:10.1016/j.bmc.2007.05.063
46. Macaeve F, Ribkovskaia Z, Pogrebnoi S, et al. The structure-antituberculosis activity relationships study in a series of 5-aryl-2-thio-1,3,4-oxadiazole derivatives. *Bioorganic & medicinal chemistry*. 2011;19(22):6792-6807. doi: 10.1021/ci010379o
47. Kubinyi H. 3D QSAR in drug design: volume 1: Theory methods and applications. vol 1. *Springer Science & Business Media*; 1993. doi:10.1021/jm010858e
48. Tetko IV. Neural Network Studies. 4. Introduction to associative neural networks. *Journal of Chemical Information and Computer Sciences*. 2002/05/01 2002;42(3):717-728. doi: 10.1021/ci00027a006
49. Tetko IV, Kovalishyn VV, Livingstone DJ. Volume learning algorithm artificial neural networks for 3D QSAR studies. *Journal of Medicinal Chemistry*. 2001;44(15):2411-2420.
50. Tetko IV, Livingstone DJ, Luik AI. Neural network studies. 1. Comparison of overfitting and overtraining. *Journal of Chemical Information and Computer Sciences*. 1995;35(5):826-833.
51. Frish MJ et al. Gaussian 09. 2009, Gaussian, Inc. Wallingford, CT, USA.
52. Becke AD. Density-functional thermochemistry. III. The role of exact exchange. *The Journal of Chemical Physics*. 1993;98(7):5648-5652. doi: 10.1063/1.464913
53. Lee CT, Yang WT, Parr RG. Development of the Colle-Salvetti correlation-energy formula into a functional of the electron-density. *Physical Review B*. 1988;37(2):785-789. doi:10.1103/PhysRevB.37.785
54. Molecular Operating Environment (MOE) CCGI, 1010 Sherbooke St. West, Suite #910, Montreal, QC, Canada, H3A 2R7, 2014